European Journal of Medicinal Chemistry 237 (2022) 114342

Contents lists available at ScienceDirect

European Journal of Medicinal Chemistry

journal homepage: http://www.elsevier.com/locate/ejmech

The role of the maleimide ring system on the structure-activity relationship of showdomycin

Petja Rosenqvist [a], Janne J. Mäkinen [b], Kaisa Palmu [b], Johanna Jokinen [b], Ranjit K. Prajapati [b], Heidi J. Korhonen [a], Pasi Virta [a], Georgiy A. Belogurov [b], Mikko Metsä-Ketelä [b, *]

[a] Department of Chemistry, University of Turku, FIN-20500, Turku, Finland
[b] Department of Life Technologies, University of Turku, FIN-20014, Turku, Finland

ARTICLE INFO

Article history:
Received 27 October 2021
Received in revised form
21 March 2022
Accepted 31 March 2022
Available online 11 April 2022

Keywords:
C-nucleosides
RNA polymerase
Transcription
Antimicrobial compounds
Streptomyces

ABSTRACT

Showdomycin produced by *Streptomyces showdoensis* ATCC 15227 is a C-nucleoside microbial natural product with antimicrobial and cytotoxic properties. The unique feature of showdomycin in comparison to other nucleosides is its maleimide base moiety, which has the distinct ability to alkylate nucleophilic thiol groups by a Michael addition reaction. In order to understand structure-activity relationships of showdomycin, we synthesized a series of derivatives with modifications in the maleimide ring at the site of alkylation to moderate its reactivity. The showdomycin congeners were designed to retain the planarity of the base ring system to allow Watson–Crick base pairing and preserve the nucleosidic character of the compounds. Consequently, we synthesized triphosphates of showdomycin derivatives and tested their activity against RNA polymerases. Bromo, methylthio, and ethylthio derivatives of showdomycin were incorporated into RNA by bacterial and mitochondrial RNA polymerases and somewhat less efficiently by the eukaryotic RNA polymerase II. Showdomycin derivatives acted as uridine mimics and delayed further extension of the RNA chain by multi-subunit, but not mitochondrial RNA polymerases. Bioactivity profiling indicated that the mechanism of action of ethylthioshowdomycin was altered, with approximately 4-fold reduction in both cytotoxicity against human embryonic kidney cells and antibacterial activity against *Escherichia coli*. In addition, the ethylthio derivative was not inactivated by medium components or influenced by addition of uridine in contrast to showdomycin. The results explain how both the maleimide ring and the nucleoside nature contribute to the bioactivity of showdomycin and demonstrates for the first time that the two activities can be separated.

1. Introduction

Nucleoside analogues currently approved for use as antiviral, antimicrobial and anticancer agents belong to the group of N-glycosides. However, because of partial hydrolysis (and phosphorolysis) of the N-glycosidic bond that occurs in biological systems and results in loss of bioactivity [1], there is an increasing interest towards natural and synthetic C-nucleosides. The carbon-carbon bond between the glycone and aglycone of C-nucleosides is resilient towards cleavage, and hence the C-nucleosides could show great potential as hydrolytically more stable nucleoside/tide drug candidates [2,3]. Potent C-nucleosides can be exemplified by pseudouridimycin [4], remdesivir [5], and an imino-C-nucleoside immucillin A [6] that inhibit bacterial or viral RNA polymerases (Fig. 1).

The broad-spectrum antibiotic showdomycin (**1**) is structurally related to uridine and pseudouridine (Fig. 1). Like uridine, **1** is complementary to adenine offering the imide face, but the pyrimidine moiety is replaced by the 5-membered maleimide ring, connected to the ribose via a C–C- bond. Maleimides are known as strong Michael acceptors for thiol and amine nucleophiles and the biological activity of **1** can be largely attributed to its reactivity with free thiol groups of cysteine residues in enzymes [7,8].

The broad-spectrum activity of **1** is evident from efficacy against Gram-positive and Gram-negative bacteria, Ehrlich ascites tumours *in vivo* and cultured HeLa cells [9,10]. Compound **1** is actively taken up into cells by membrane nucleoside transporters [11], but

* Corresponding author.
E-mail address: mianme@utu.fi (M. Metsä-Ketelä).

https://doi.org/10.1016/j.ejmech.2022.114342

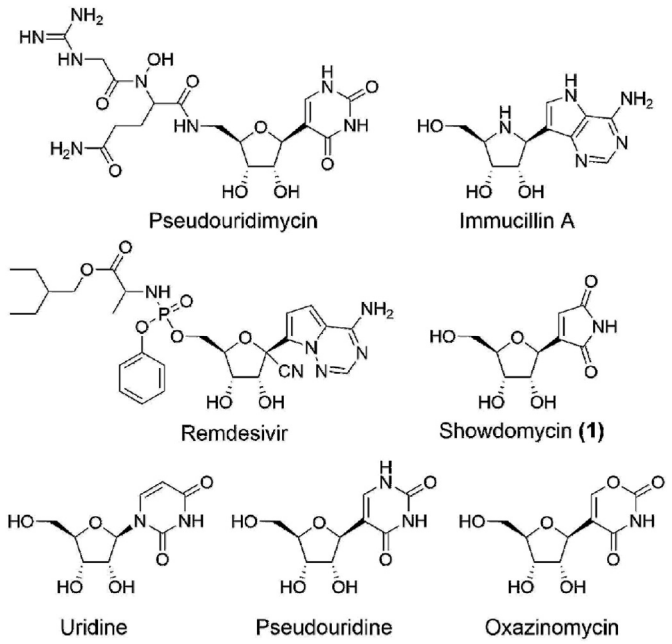

Fig. 1. Structures of pseudouridimycin, remdesivir, immucillin A, showdomycin (1), uridine, pseudouridine and oxazinomycin. The unique feature of **1** is the highly reactive maleimide ring system.

inhibition of the transporter enzymes by **1** on cancer cells has also been observed [11,12]. The mechanism of action of **1** has remained elusive, since a wide variety of cellular targets have been reported. *In vitro*, **1** has been reported to inhibit enzymes such as UMP kinase, uridine phosphorylase, UDP-glucose dehydrogenase and (Na^++ K^+)-ATPase in mammalian cells as well as thymidylate synthetase in *E. coli* (12) [7,13,14]. *In vivo* target analysis performed on *Staphylococcus aureus* bacteria with a showdomycin probe containing a hexynoic acid ester modification at 5′-hydroxyl, which allows tagging by azide-alkyne click chemistry, revealed a variety of potential target enzymes. Interestingly, many of the identified enzymes utilized nucleoside based natural substrates [15], which indicates that both the nucleoside character and the alkylating capability of **1** are major contributors to its activity.

Another key question is whether the biological activity of **1** occurs as a nucleoside or a nucleotide. In contrast to most nucleoside-based antibiotics, **1** was not phosphorylated *in vitro* by nucleoside kinases reflecting bioactivities of the non-phosphorylated nucleoside [7]. However, evidence of intracellular phosphorylation of **1** has been detected in mouse lymphoma cells [16] and, additionally, increased inhibition of thymidylate synthetase *in vitro* by showdomycin-5′-phosphate in comparison to **1** has been noted [14]. Therefore, the significance of possible intracellular phosphorylation of **1** and its influence on cellular processes (e.g. transcription) are currently unknown.

Bacterial RNA polymerase (RNAP) is a potential drug target and several classes of selective RNAP inhibiting drugs have been described [17,18]. As an example of nucleotide mimics, pseudouridimycin has been shown to target the nucleotide addition site of bacterial RNAP [4], while oxazinomycin (Fig. 1) triphosphate is able to arrest RNAP at polythymidine sequences *in vitro* [19]. It has been suggested that **1** interacts and inhibits the DNA-free form of RNAP [20], possible via interactions of the maleimide group, since pre-incubation with **1** was required for inhibitory effects against *E. coli* RNAP *in vitro*. However, interactions of phosphorylated **1** or its analogues on RNAP elongation complexes and their plausible nucleobase-specific effect on the active site have not yet been studied.

We postulated that the diverse biological activities of **1** could be influenced by separation of the bioactivities resulting from the general nucleoside character of the molecule and the reactive maleimide ring system. In order to understand the structure-activity relationships of this unique C-nucleoside, here we report the semisynthetic preparation of base-modified showdomycin-5′-triphosphates and the assessment of their actions on transcription by multi- and single-subunit RNAPs. We further show that inactivation of the maleimide ring decreases the antimicrobial and cytotoxic activities *in vivo*, and appears to alter the mode of action of the showdomycin derivatives.

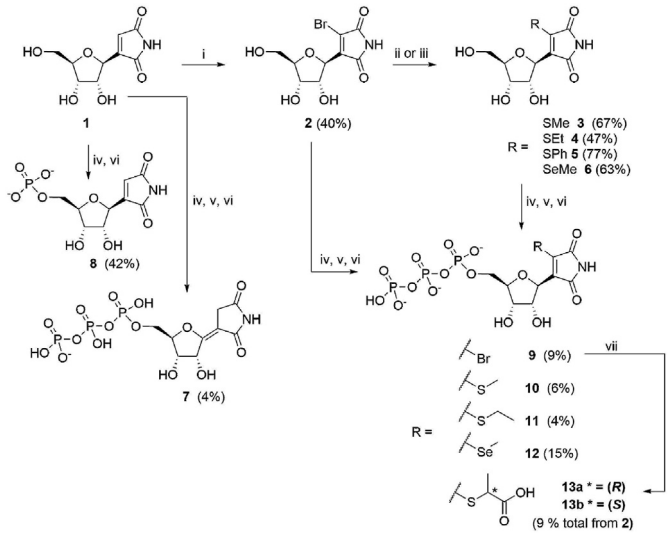

Scheme 1. Synthesis of showdomycin analogues and generation of triphosphate congeners.
Reagents and conditions: (i) Br_2, Fe (s), H_2O, RT, 72 h; (ii) MeSNa or EtSH or PhSH, DIEA, THF, RT, 4–20 h; (iii) MeSeSeMe, $NaBH_4$, EtOH/DMF, 0 °C – RT, 40 min; (iv) $POCl_3$, 2,4,6-trimethylpyridine, triethyl phosphate, - 10 °C – 4 °C, 1.5–20 h; (v) tris(tetrabutylammonium) hydrogen pyrophosphate, tributylamine, 0 °C – RT, 20 h; (vi) 0.05 M triethylammonium acetate, $CHCl_3$, RT, 30 min; (vii) thiolactic acid, DIEA, triethylphosphate/DMSO, RT, 4 h.

2. Results

Semisynthesis of showdomycin analogues. Production of showdomycin (**1**) by cultivating *S. showdoensis* ATCC 15227 and its isolation were carried out by methods described earlier [21,22]. After 20 h cultivation, the concentration of **1** reached 150–180 mg/l, and the compound was extracted with activated charcoal and purified by silica column chromatography.

Preparation of showdomycin analogues (**2**–**7**) by modifying the base moiety is depicted in Scheme 1. The α,β-unsaturated carbonyl structure of the maleimide base was desired to be present in the analogues in order to retain a degree of the biologically relevant reactivity of **1**. Therefore, **1** was first treated with bromine in the presence of a catalytic amount of iron powder to obtain 4-bromoshowdomycin (**2**). Michael addition to **2** with sodium thiomethoxide, ethanethiol, thiophenol or methaneselenol in presence of a base, followed by spontaneous elimination of the bromide group afforded 4-methylthioshowdomycin (**3**), 4-ethylthioshowdomycin (**4**), 4-benzenethioshowdomycin (**5**) and 4-methylselenoshowdomycin (**6**), respectively.

The nucleosides were synthetically transformed into 5′-triphosphates using the Ludwig-modified Yoshikawa method, i.e. by treating the unprotected nucleosides with phosphoryl chloride in

trialkyl phosphate solvent and subsequently with tris(tetrabutylammonium) hydrogen pyrophosphate [23]. Unexpectedly, the triphosphorylation of **1** and the following HPLC purification afforded the isomerized product, *iso*-showdomycin-5′-triphosphate (**7**). Similar isomerization has been reported to be catalysed by an enzyme isolated from showdomycin resistant *Streptomyces* strain (sp. 383) [24]. However, the isomerization did not occur when the pyrophosphate treatment was omitted in order to synthesize showdomycin-5′-monophosphate (**8**).

The analogues **2**–**6** retained their structural configuration under the triphosphorylation conditions. However, the 4-bromo-showdomycin-5′-triphosphate (**9**) was prone to hydrolysis during RP-HPLC purification with buffered eluents. As an alternative, the crude product of **9** was treated with pyrophosphatase to remove the pyrophosphate impurity and the phosphorylated compound was subsequently precipitated as a sodium salt from acetone to obtain sufficient purity for RNAP assays. On the other hand, the 5′-triphosphate of the benzenethiol modified analogue **5** proved to be unstable in solution and degraded during the HPLC purification. In contrast, the 4-methylthioshowdomycin-5′-triphosphate (**10**) and 4-ethylthioshowdomycin-5′-triphosphate (**11**) were obtained as stable triethylammonium salts and the 4-methylselenoshowdomycin-5′-triphosphate **13** was precipitated as a sodium salt after HPLC purification to avoid possible degradation.

The thiol groups could also be introduced to the maleimide moiety after the triphosphorylation. Accordingly, a reaction of the triphosphate **9** with a racemic mixture of thiolactic acid yielded the 4-((1-carboxyethyl)thio)showdomycin-5′-triphosphate diastereomers **13a** and **13b** that were separated by HPLC and identified by comparing to a pure sample of **13b** that was prepared in small scale with enantiopure (2*S*)-thiolactic acid.

RNA polymerases incorporate 4-ethylthioshowdomycin into RNA in place of uridine. We first tested if **11** can be incorporated into RNA in place of uridine by the multi-subunit RNAP from *E. coli* (*Eco*), RNA polymerase II from *S. cerevisiae* (*Sce* RNAPII) and the single-subunit RNAP from human mitochondria (*Hsa* MT RNAP). Transcription elongation complexes (TEC) were assembled on synthetic nucleic acid scaffolds and contained a fully complementary transcription bubble flanked by 20-nucleotide long DNA duplexes upstream and downstream (Fig. 2A). The annealing region of a 16-nucleotide RNA primer was 9 nucleotides. The RNA primer was 5' labeled with the infrared fluorophore ATTO680 to monitor RNA extension by denaturing PAGE. We first employed an *Eco* RNAP TEC that incorporates uridine followed by guanosine. The addition of UTP and UTP + GTP to the TEC resulted in extension of the TEC by one and two nucleotides, respectively (Fig. 2A, *lanes 1*–*3*). The employment of **11** in place of UTP resulted in the extension of the TEC by one nucleotide, but further extension in the presence of GTP was very inefficient (Fig. 2A, *lanes 4*–*5*). *Sce* RNAPII TEC was less efficient than *Eco* RNAP TEC in incorporating 4-ethylthioshowdomycin-5′-monophosphate (**14**) into RNA when **11** was used as a substrate and no further extension by GMP was observed during the timeframe of the experiment (1 min). Finally, *Hsa* MT RNAP TEC was efficiently extended by one nucleotide in the presence of **11** and by two nucleotides in the presence of **11** and GTP. None of the RNAPs in our test incorporated **14** in place of cytidine, adenine or guanine (Fig. 2B). Taken together, these results suggested that **11** is exclusively a UTP analogue.

Effect of 4-ethylthio-showdomycin and other showdomycin derivatives on processive transcription elongation. We next tested if other triphosphorylated showdomycin derivatives can serve as substrates for *Eco* RNAP, *Sce* RNAPII and *Hsa* MT RNAP (Supplementary Fig. 1). All RNAPs in our set were able to utilize 4-bromo-, 4-methylthio- and 4-methylseleno-showdomycin triphosphates (**9**, **10** and **12**) in place of UTP, whereas only *Eco* RNAP TEC was able to utilize the 4-(1-carboxyethyl)thio-showdomycin-5′-triphosphate isomers **13a** and **13b**.

We then examined if **11** and other triphosphorylated derivatives can inhibit processive transcription elongation by *Eco* RNAP, *Sce* RNAPII and *Hsa* MT-RNAP. The synthetic nucleic acid scaffold contained a fully complementary transcription bubble flanked by 12- and 49-nucleotide long duplexes upstream and downstream, respectively. We utilized a DNA template containing an 11-nucleotide-long thymidine-free leader followed by a sequence of 7 consecutive thymidines (positions 12 to 18 downstream from the RNA primer) to investigate the efficiency of incorporation of uridines or uridine analogues into RNA during transcription (Fig. 3). The DNA template also contained several other U-encoding positions downstream of the polythymidine tract (positions 23, 27, 32, 35, 37, 41 and 47 downstream from the RNA primer).

We performed transcription at 100 μM of natural substrates (ATP, CTP, GTP and UTP) and 2000 μM of triphosphorylated showdomycin derivatives to maximise the effect of the latter on transcription of a relatively short template. The probability of the incorporation of a showdomycin derivative into RNA is approximately proportional to the number of U-encoding positions under the conditions of the experiment (competition with UTP). Accordingly, incorporation-proficient showdomycin derivatives are expected to exert effects on RNA synthesis at progressively lower concentrations as the length of RNA increases and inhibit transcription by slowing down the incorporation of the next nucleotide.

Showdomycin derivatives with small functional groups at C4 of the base moiety (**9**, **10**, **11**, **12**) inhibited processive transcript elongation by *Eco* RNAP with **11** having the strongest effect: **11** increased the fraction of the *Eco* RNAP paused at the polythymidine tract nearly 3-fold whereas **9**, **10** and **12** doubled the amount of *Eco* RNAP delayed at the polythymidine tract (Fig. 3, left). The inhibition was likely due to RNAP pausing after the incorporation of a showdomycin derivative, since the presence of the latter in the reactions increased the amount of RNA at the U-encoding sites rather than before the U-encoding sites. We observed similar though apparently less potent effects of **9**, **10**, **11** and **12** on the *Sce* RNAPII (Fig. 3, middle). The interpretation of the latter observations was complicated because *Sce* RNAPII transcribed a polythymidine tract inefficiently also in the absence of showdomycin derivatives. In contrast, **9**, **10**, **11**, **12** did not measurably delay the *Hsa* MT RNAP at U-encoding positions (Fig. 3, right), consistently with the observations that MT-RNAP efficiently extended incorporated showdomycin derivatives in single-nucleotide addition experiments (Fig. 2A, Supplementary Fig. 1).

We also included incorporation-deficient derivatives into the test to test their potential as competitive inhibitors. However, the incorporation-deficient showdomycin derivatives (**13a**, **13b**) did not measurably affect processive transcription by any enzyme in our set, suggesting that these derivatives did not bind to the RNAP active sites sufficiently tight to act as competitive inhibitors.

Antibacterial activity of showdomycin analogues. Next we evaluated the biological activity of 1 and the lead compound **4** *in vivo* against *E. coli*. We utilized the reporter strain *E. coli*/p*lux*, which expresses bacterial luciferase *luxA* and *luxB*, and harbors genes *luxC*, *luxD* and *luxE* for production of fatty aldehyde substrates *in situ*. Bacterial luciferase biosensors provide a convenient indicator for the metabolic state of the cell by utilizing reduced flavin mononucleotide (FMN/FMNH2) for oxidation of long-chain fatty aldehydes, with concomitant bioluminescence emission at 490 nm [25]. Optical density OD_{600} measurements were used to monitor total cell populations (Fig. 4, *dotted lines*), whereas the bioluminescence signal (Fig. 4, *solid lines*) was used to estimate the

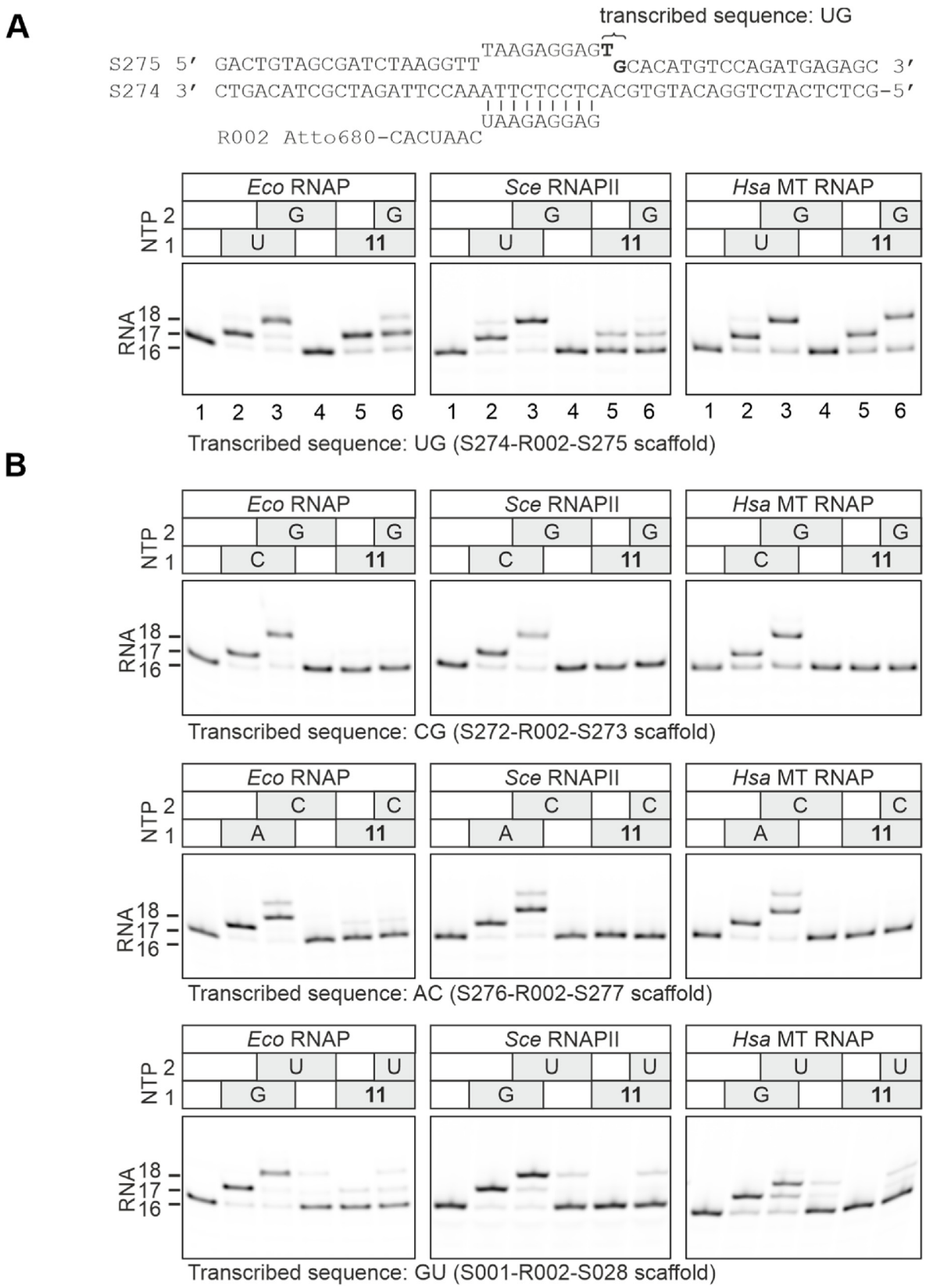

Fig. 2. ***Eco*** **RNAP,** ***Sce*** **RNAPII and** ***Hsa*** **MT RNAP can utilize 11 as a substrate to incorporate 14 into RNA in place of uridine.** (A) Incorporation of **14** in place of uridine: the initial TECs (lanes 1 and 4) were supplemented with UTP and GTP (lanes 2–3) or **11** and GTP (lanes 5–6). The nucleic acid scaffold employed in the experiments is depicted above gel panels. NTPs (20 μM) and 11 (100 μM) were added and the reactions were incubated for 1 min at 25 °C. (B) Incorporation of **14** in place of cytidine, adenine and guanine. The employed nucleic acid scaffolds had same overall architecture as the scaffold depicted in (A) but differed in the transcribed sequence immediately downstream of the RNA primer. Fractional misincorporations (additional bands) are evident in several lanes.

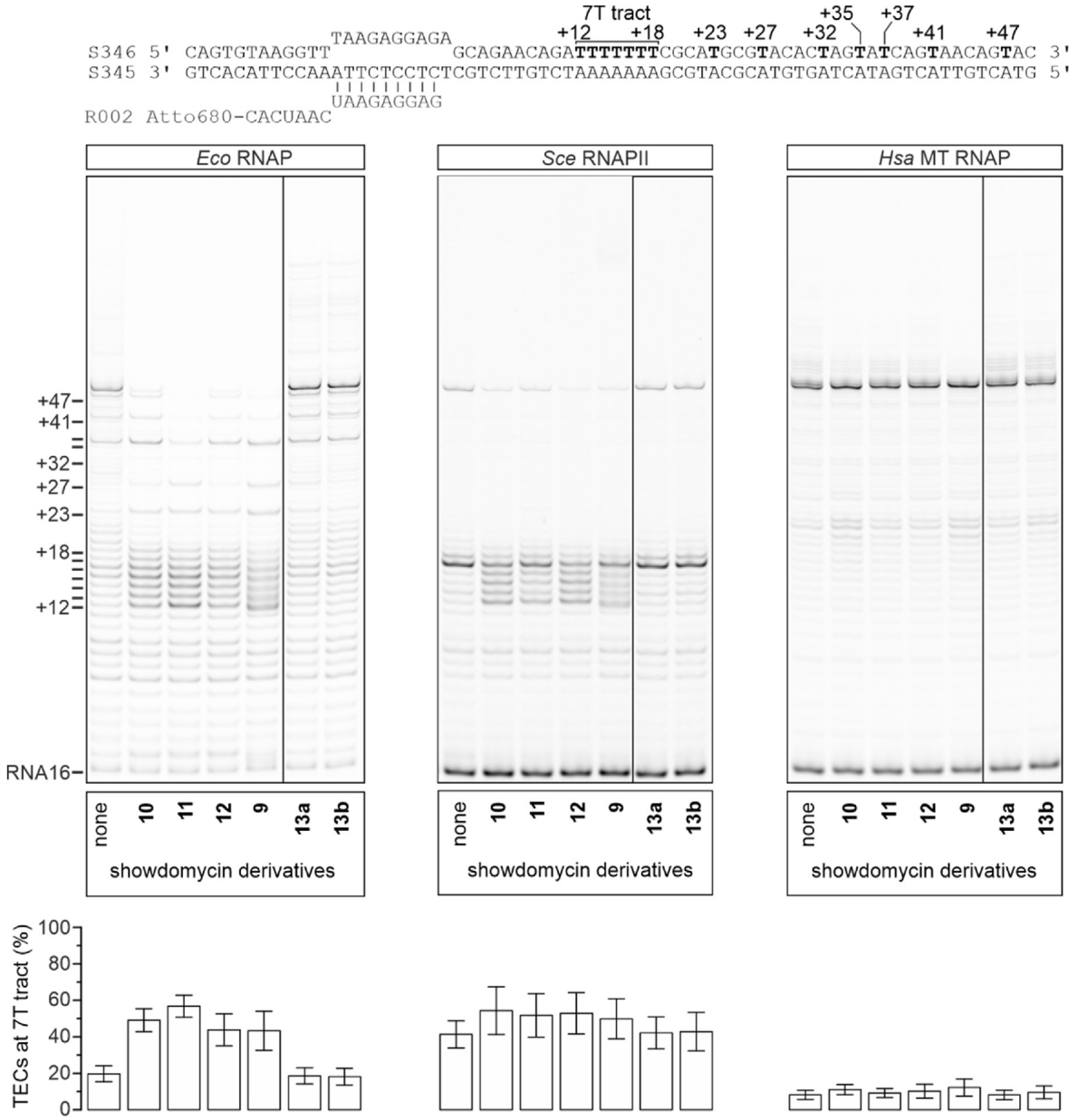

Fig. 3. The effects of 5′ triphosphorylated showdomycin derivatives on processive transcription elongation by *Eco* RNAP (left), *Sce* RNAPII (middle) and *Hsa* MT RNAP (right). The nucleic acid scaffold employed in the experiments is depicted above gel panels. ATP, CTP, GTP, UTP (100 μM each) and showdomycin derivatives (2 mM) were added, and the reactions were incubated for 5 min at 25 °C. Bar graphs below the gel panels display fractions of RNAPs delayed at the polythymidine tract (positions +12 to +18). A single lane between compounds **9** and **13a** was spliced out from each gel panel as indicated by black vertical lines.

redox state and metabolic activity of live cells. The experiments were conducted on microtiter plates using known antibiotics kanamycin, apramycin and pseudouridimycin as controls (Fig. 4A–C). Kanamycin and apramycin bind to the 30S ribosomal subunit leading to misreading of RNA and incorporation of wrong amino acids into proteins. In the assay, inhibition of growth was observed by a steep decline in optical density and luminescence by both antibiotics at a threshold concentration of around 40 μM (Fig. 4A and B). In contrast, pseudouridimycin is a competitive inhibitor of RNA polymerase [4] and the concentration dependent antibiotic effect was readily observable from both OD_{600} and luminescence measurements (Fig. 4C).

The growth inhibition curve for **1** (Fig. 4D) was found to display similarity to both kanamycin/apramycin and pseudouridimycin control groups, but the growth inhibition induced by 4 (Fig. 4E) is highly reminiscent of the profile for pseudouridimycin. The optical density measurements confirmed that **4** functioned as an antibiotic and inhibited the growth of *E. coli*/p*lux*, but to a lesser extent in comparison to **1**. We observed a rapid decline of the luminescence signal indicating bacteriocidal activity [25] at a concentration of 0.625 mM with **1**, whereas 2.5 mM of 4 was needed to induce the same effect. Interestingly, cells treated with low concentrations of **1** were able to recover from the growth inhibitory effect and an increase in metabolic activity was detected at around 250 min (Fig. 4D). The maleimide ring of **1** has been reported to react with culture medium components [7,26], which may explain the loss of activity of the molecule. It is noteworthy that a similar increase in luminescence was not observed with **4** (Fig. 4E), where the

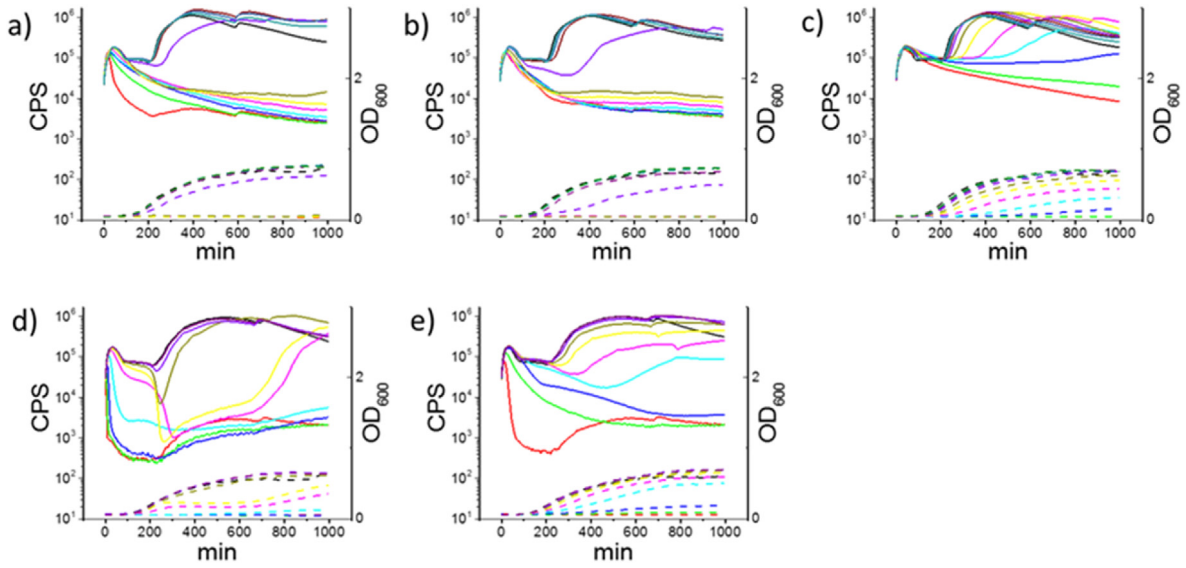

Fig. 4. Evaluation of antibiotic efficacy of 1 and 4 by optical density and bioluminescence in *E. coli*/*plux*. Growth inhibition curves for a) the control antibiotic apramycin b) the control antibiotic kanamycin, c) competitive control antibiotic pseudouridimycin, d) **1** and e) **4**. Solid line: luminescence in counts per second (CPS) and dotted line: OD_{600}. Concentrations of analytics are depicted in different colors: red, 2.5 mM; green, 1.25 mM; blue, 0.625 mM; cyan, 0.3125 mM; pink, 0.156 mM; yellow, 0.078 mM; dark yellow, 0.039 mM; violet, 0.020 mM; ruby red, 0.010 mM; dark cyan, 0.005 mM; olive, 0.002 mM; black, no analytic added (control).

thioethyl substituent decreases the reactivity of the maleimide ring system.

It has been reported that the inhibitory activity of **1** can be reversed by addition of canonical nucleosides [26], which outcompete membrane nucleotide transporters and prevent entry of **1** into cells [27]. In our assay, we were able to observe the reversal effect at equimolar concentrations of uridine and **1** in both the OD_{600} and bioluminescence measurements (Supplementary Figs. 2A–B), whereas uridine had hardly any effect on the activity of **4** under similar conditions (Supplementary Figs. 2C–E). The effect was even more pronounced at fivefold uridine concentrations with **1** (Fig. 5A and B), yet the reversal of inhibition of **4** remained minimal and could also be explained by increase of growth rate by uridine (Fig. 5C–E).

Cytotoxicity of showdomycin analogues. The biological activity of **1** and **4** was also assayed against human embryonic kidney 293T (ACC 635) cell lines to determine cytotoxicity profiles. Cell death was tracked with a lactate dehydrogenase (LDH) cytotoxicity assay kit, which revealed cellular toxicity for **1** and **4** at concentrations of approximately 30 μM and 125 μM, respectively (Fig. 6A). In addition, the influence of **1** and **4** on cell proliferation was estimated with the Cell Counting Kit-8 (CCK-8), which confirmed the reduced toxicity of **4** (Fig. 6B). The cell viability data provided additional support for the altered mechanism of action for **4** that was detected in the antimicrobial assays; the number of viable cells was drastically reduced in cells treated with **1** already at 125 μM,

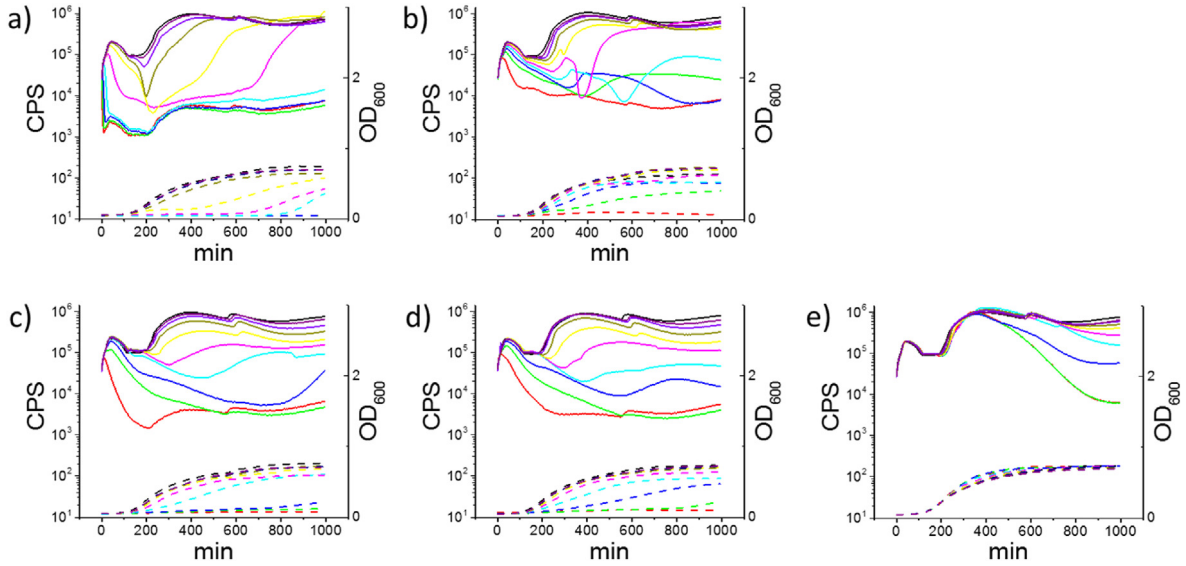

Fig. 5. Influence of uridine supplementation on the antimicrobial activity of 1 and 4. Growth inhibition curves for a) **1**, b) **1** in the presence of five-fold excess of uridine, c) **4** and d) **4** in the presence of five-fold excess of uridine, e) uridine. The concentrations of the nucleosides are color-coded as in Fig. 4.

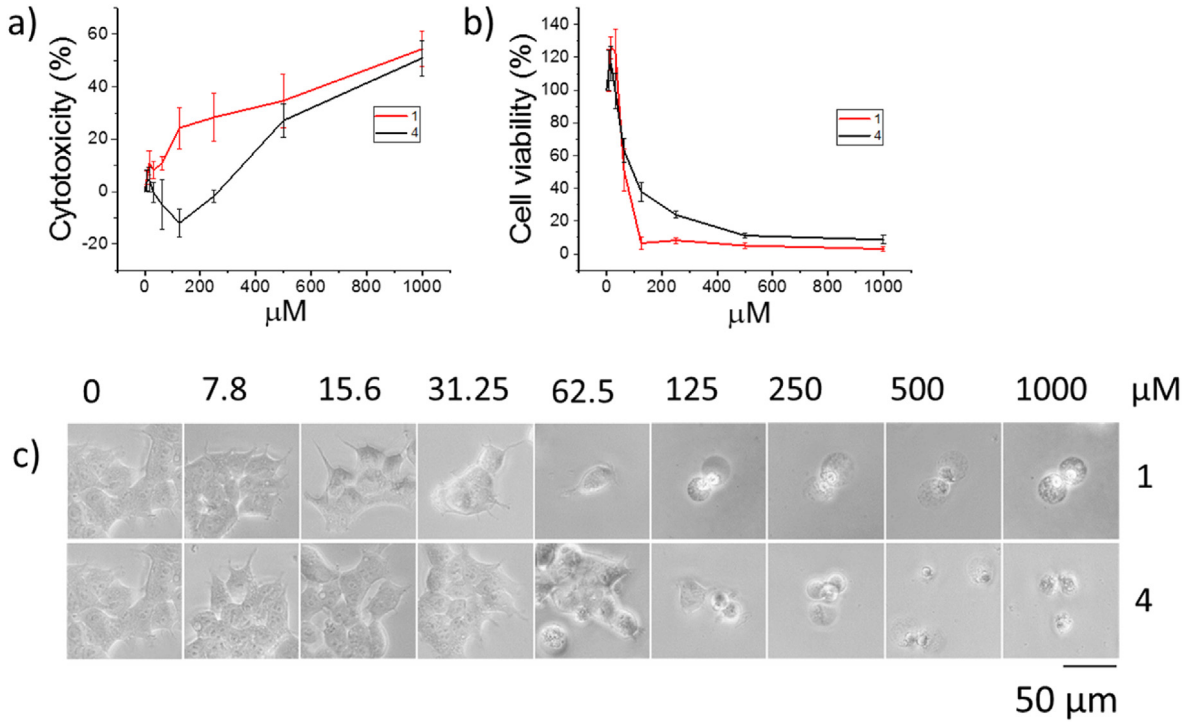

Fig. 6. Cytotoxicity profiles of 1 and 4. Determination of a) cell lysis by LDH-cytotoxicity assay and b) cell viability by Cell Counting Kit-8 with varying concentrations of **1** and **4**. The data are shown as the mean ± SD from three independent experiments. c) The influence of **1** and **4** on the morphology of human embryonic kidney cell line 293T.

whereas a much higher concentration of **4** at approximately 500 μM was required to reach a similar effect on cell viability. It is noteworthy that the concentration range where the cytotoxicity of **1** and **4** could be detected in the assays correlated well with morphological changes observed in the cells at 30 μM and 125 μM, respectively (Fig. 6C).

3. Discussion

The biological activity of the natural C-nucleoside showdomycin (**1**) is contributed by two factors, the alkylating nature of the maleimide-type nucleobase and the overall nucleosidic structure of the molecule. This has led to the identification of several cellular targets and complicated identification of the toxicity issues associated with **1** [7,10,15]. In the current study, we introduced various modifications to the maleimide moiety of **1** in order to mitigate its reactivity. We then explored the feasibility of the derivatives to function as RNA polymerase substrates. The nucleotide analogues containing bromo- (**9**), methylthio- (**10**), ethylthio- (**11**) or methylseleno- (**12**) modifications at the maleimide C-4, were incorporated to the nascent RNA in place of uridine and furthermore, were able to partially inhibit further elongation by the multi-subunit RNA polymerases. In addition, the observed inhibition was slightly more efficient against bacterial multi-subunit RNAP compared to the eukaryotic one. On the other hand, incorporation of the nucleotides **9**–**12** by the single-subunit (human mitochondrial) RNAP did not results in observable inhibition. When tested against processive transcription by multi-subunit RNAPs, the presence of nucleotides **9**–**12** caused fractional arrests at the positions of incorporation, but no evidence of delayed chain termination was observed. Again, the inhibitory effect was uniquely observed in case of the multi-subunit polymerases and was attributed to pausing of the elongation complex upon incorporation of the unnatural nucleotides. The most distinguishable effect on transcription was observed with the 4-ethylthio-showdomycin-5′-triphosphate (**11**). On the other hand, the analogues with larger substituents (i.e 4-(1-carboxyethyl)thio (**13a** and **13b**) modifications) possessed negligible activity and were most likely not able to bind to the nucleotide addition site. Due to the isomerization of unmodified **1** during the chemical phosphorylation, no conclusion can be made on whether the base-modifications increase or decrease the RNAP activity compared to the hypothetical unmodified showdomycin-5′-triphosphate.

We were able to gain insight into the differences in antimicrobial activities between **1** and our lead compound, 4-(ethylthio) showdomycin (**4**) by utilizing the reporter strain *E. coli*/p*lux*. Although the bacterial growth inhibition by **4** was 4-fold less effective compared to **1**, the inhibition capability of **4** was not diminished by the presence of uridine in contrast to **1**. This observation suggests that the entry of **4** into bacterial cells is not competed by uridine. Alternatively, the supplemented uridine may have a protective effect against **1**, if the mechanism of action of **1** includes inhibition of enzymes involved in uridine metabolism. In addition, the observed loss of bioactivity of **1**, presumed to stem from interactions of the maleimide and medium components, was not detected with **4.** The modifications reduced the cytotoxicity of **4** to human embryonic kidney cells also approximately 4-fold in comparison to **1**, which would indicate that the reduced bioactivity due to the loss of the maleimide ring system of **1** occurs similarly both in prokaryotes and eukaryotes.

One highly interesting aspect is the effect of the 4-(ethylthio) group on the pharmacodynamics of **1** and **4**, which is evident from the shapes of the bioluminescence curves that reflect the metabolic activity of the bacteria. Compound **1** displayed growth inhibition properties similar to kanamycin and apramycin (Fig. 4A–D), whereas the profile for **4** was found to be concentration dependent and highly reminiscent to the graphs of the competitive RNA polymerase inhibitor pseudouridimycin (Fig. 4C and **E**). The same effect is apparent in cell viability assays (Fig. 6B), where **1** induced cell death abruptly after a threshold concentration value of

approximately 125 μM, whereas **4** behaved in a more concentration dependent manner, as is evident from the hyperbolic shape of the graph towards 500 μM.

In conclusion, we have utilized a facile semisynthetic method to prepare a small library of base-modified showdomycin analogues. We showed that the relatively simple modification alters the mechanism of action of **1**, as well as protects the compound from loss of bioactivity *in vivo*. The lower efficacy of **4** in comparison to **1** in the antimicrobial and cytotoxicity assays may be explained by reduced reactivity of the maleimide base, which implies that **4** may have fewer cellular targets and functions solely as a nucleoside analogue to mediate its biological effect. Unfortunately, the level of intracellular phosphorylation of the prepared showdomycin analogues is unknown and therefore, the RNAP inhibition activity of the nucleotide **11** cannot be directly linked to the observed activity of the nucleoside **4**. The relatively low efficacy of **11** as an RNAP substrate implies that the RNAP inhibition may not be the principal mechanism of action causing the observed antimicrobial activity. However, the observed inhibitory activity could serve as a lead for designing selective inhibitors of bacterial RNAP. In addition, future investigations into the biological activity of **4** may provide insight into the multifaceted mechanism of action of **1** via dissection of the structure-activity relationships that originate either from the reactivity of the maleimide ring system or the general nucleosidic nature of the compound. Our data suggests that both properties contribute to the antimicrobial activities and cytotoxicity of the compounds and demonstrates for the first time that these activities can be separated. The potent bioactivities and resistance to hydrolysis has reinvigorated interest in both synthetic and biosynthetic C-nucleosides in recent years [2,3,28]. The work presented here provides a platform for synthesis and analysis of C-nucleoside analogues to be expanded in our laboratories in the future.

4. Materials and methods

Reagents and oligonucleotides. HPLC purified DNA oligonucleotides were purchased from Eurofins Genomics GmbH (Ebersberg, Germany). The PAGE purified ATTO-680 labeled RNA primer was purchased from IBA Biotech (Göttingen, Germany). NTPs were from Jena Bioscience (Jena, Germany). All other reagents used were molecular biology grade.

General. The NMR spectra were recorded with a Bruker Avance 500 MHz spectrometer. The high resolution mass spectra were recorded with a Bruker Daltonics microTOF-Q instrument. LC-MS was recorded on an Agilent 1260 Infinity Binary LC and Agilent 6100 Series Quadropole mass spectrometer with a Phenomemex 150 × 4.6 Synergi™ 4 μm Fusion-RP 80 Å. All compounds are >95% pure by HPLC analysis.

Showdomycin concentration analysis. The concentration of **1** was assayed as was established earlier [21]. **1** in the sample was consumed by a known excess of glutathione (GSH) and the remaining GSH was derivatized with Ellman's reagent, 5,5′-dithiobis(2-nitrobenzoic acid) (DTNB) and measured by spectrophotometry. For the assay, a sample containing **1** (10–100 μl) was mixed to a solution of GSH (3.65×10^{-5} M) in 0.1 M potassium phosphate buffer at pH 7.27 containing 1 mM EDTA and the reaction was allowed to proceed at room temperature for 5 min. A solution of DTNB (10 μl) was added and the reaction was incubated for 1 min at room temperature and the absorbance of the GSH-DTNB product was measured at 412 nm. The molar amount of GSH reacted with **1** was then calculated using a molar extinction coefficient of 14150 M^{-1} cm^{-1} [29].

Production of showdomycin (1). Cultivation of *S. showdoensis* ATCC 15227 and isolation of **1** were carried out by a slightly modified method described earlier. The growth medium containing 5 g/L potato starch, 5 g/L glycerol, 5 g/L glucose, 5 g/L peptone, 4 g/L potato juice and 3 g/L NaCl in mQ water was used to prepare a preculture by inoculating the medium (70 ml) with *S. showdoensis* ATCC 15227 grown on a plate and incubating on a reciprocal shaker for 72 h at 30 °C. The preculture (40 ml) was used to inoculate 4 L of the same type of growth medium in a Biostat B bioreactor which was being aerated for 6 L/min, mixed at 250 rpm and maintained at 30 °C for the duration of the production. The concentration of **1** in the culture was monitored using the method described above. When the concentration of **1** reached 150–180 mg/L, the broth was centrifuged, and the supernatant was collected and adjusted to pH 5.0 with 1 M hydrochloric acid. Activated charcoal powder (20 g/L) was added and the mixture was stored at 4 °C overnight. The charcoal was filtered and extracted with acetone/water (8:2) (1 l) and the extracts were evaporated to near dryness under reduced pressure. The residue was extracted with methanol and the extracts were concentrated to a small volume and applied to a column of silica gel packed with toluene. The column was eluted first with 200 ml of acetone/toluene (1:4) and then with acetone/toluene (4:1). Fractions containing **1** were evaporated to dryness and further purified by silica gel chromatography with DCM/MeOH (9:1, *v/v*). The product fractions were evaporated to dryness yielding **1** (435 mg) as a white crystalline solid. ^{1}H NMR δ_H (500 MHz, D_2O): 6.65 (d, J = 1.7 Hz, 1H), 4.74 (dd, J = 1.7 and 4.7 Hz, 1H), 4.21 (pseudo-t, J = 4.7 Hz, 1H), 4.04 (dd, J = 6.1 and 4.7 Hz, 1H), 3.98 (m, 1H), 3.81–3.76 (dd, J = 3.1 and 12.6 Hz, 1H), 3.67–3.62 (dd, J = 5.2 and 12.6 Hz, 1H). ^{13}C NMR δ_C (125 MHz, D_2O): 173.1, 172.4, 147.1, 129.2, 83.2, 77.5, 74.4, 70.8, 61.3. HRMS (ESI) *m/z*: [M − H]$^-$ calcd for $C_9H_{10}NO_6^-$ 228.0514; found 228.0520.

4-Bromoshowdomycin (2). Compound **1** (300 mg, 0.97 mmol) was dissolved in water (10 ml) saturated with Br_2 and a catalytic amount of iron powder was added. The resulting solution was stirred at room temperature for 72 h, then concentrated and subjected to a RP silica column. The column was eluted with water and then with 95:5 water/acetonitrile. The product fractions were collected and concentrated to give **2** as a white crystalline solid (163 mg, 40%). ^{1}H NMR δ_H (500 MHz, D_2O): 4.82 (d, J = 6.8 Hz, 1H), 4.43 (dd, J = 5.5 and 6.8 Hz, 1H), 4.17 (dd, J = 4.4 and 5.5 Hz, 1H), 4.00 (m, 1H), 3.77–3.69 (m, 2H). ^{13}C NMR δ_C (125 MHz, D_2O): 170.0, 167.1, 139.0, 129.7, 85.0, 76.6, 73.8, 71.5, 61.7. HRMS (ESI) *m/z*: [M − H]$^-$ calcd for $C_9H_9BrNO_6^-$ 307.9619; found 307.9598.

4-Methylthioshowdomycin (3). Sodium thiomethoxide (11.5 mg, 0.16 mmol, 1 equiv) and DIEA (57 μl, 0.32 mmol, 2 equiv) were added to a solution of **2** (50 mg, 0.16 mmol) in THF (1 ml). The mixture was stirred for 4 h at room temperature and applied as such to a silica column. The column was eluted with DCM/MeOH (9:1, *v/v*). The product fractions were evaporated to dryness to give **3** as a yellow crystalline solid (30 mg, 67%). ^{1}H NMR δ_H (500 MHz, CD_3OD): 4.84 (overlap with MeOD, 1H), 4.40 (dd, J = 5.6 and 7.1 Hz, 1H), 4.14 (dd, J = 3.6 and 5.5 Hz, 1H), 3.98 (m, 1H), 3.75 (dd, J = 3.7 and 12.0 Hz, 1H), 3.66 (dd, J = 4.5 and 12.0 Hz, 1H), 2.75 (s, 3H). ^{13}C NMR δ_C (125 MHz, CD_3OD): 170.0, 168.0, 144.5, 133.2, 85.9, 76.3, 74.0, 72.4, 62.5, 13.8. HRMS (ESI) *m/z*: [M − H]$^-$ calcd for $C_{10}H_{12}NO_6S^-$ 274.0391; found 274.0399.

4-Ethylthioshowdomycin (4). Ethanethiol (28 μl, 0.39 mmol, 1.1 equiv) and DIEA (183 μl, 1.05 mmol, 3 equiv) were added to a mixture of **2** (109 mg, 0.35 mmol) in THF (2 ml) and the reaction was allowed to proceed for 20 h at room temperature. The mixture was evaporated to dryness and the residue was purified by silica gel chromatography using DCM/MeOH (95:5, v/v) as an eluent. The product fractions were combined and evaporated to dryness to give **4** as a yellow crystalline solid (48.2 mg, 47%). ^{1}H NMR δ_H (500 MHz, D_2O): 4.81 (d, J = 7.0 Hz, 1H, 4.44 (dd, J = 5.7 and 7.0 Hz, 1H), 4.17 (dd, J = 3.9 and 5.7 Hz, 1H), 4.00 (m, 1H), 3.78–3.68 (m, 2H), 3.34–3.17 (m, 2H), 1.26 (t, J = 7.4 Hz, 3H). ^{13}C NMR δ_C (125 MHz, D_2O): 170.8, 169.1, 145.0,

133.6, 85.0, 75.9, 73.4, 71.7, 61.8, 26.5, 14.9. HRMS (ESI) *m/z*: [M − H]$^-$ calcd for $C_{11}H_{14}NO_6S^-$ 288.0547; found 288.0545.

4-Phenylthioshowdomycin (5). Thiophenol (14 μl, 0.14 mmol, 1.1 equiv) and DIEA (66 μl, 0.38 mmol, 3 equiv) were added to a mixture of **2** (39 mg, 0.13 mmol) in THF (0.5 ml). The reaction was allowed to proceed for 18 h at room temperature. The mixture was evaporated to dryness and the residue was purified by silica gel chromatography using DCM/MeOH (95:5, v/v) as an eluent. The product fractions were combined and evaporated to dryness to give **5** as a yellow crystalline solid (33 mg, 77%). ^{1}H NMR δ_H (500 MHz, CD_3OD): 7.52 (m, 2H), 7.39−7.36 (m, 3H), 4.77 (d, J = 7.3 Hz, 1H), 4.43 (dd, J = 5.6 and 7.3 Hz, 1H), 4.15 (dd, J = 3.7 and 5.6 Hz, 1H), 3.94 (m, 1H), 3.76 (dd, J = 3.7 and 12.0 Hz, 1H), 3.66 (dd, J = 4.6 and 12.0 Hz, 1H). ^{13}C NMR δ_C (125 MHz, CD_3OD): 169.8, 167.1, 142.0, 139.0, 132, 130, 129, 128.3, 86.1, 76.3, 74.3, 72.4, 62.5. HRMS (ESI) *m/z*: [M − H]$^-$ calcd for $C_{15}H_{14}NO_6S^-$ 336.0547; found 336.0557.

4-Methylselenoshowdomycin (6). Dimethyldiselenide (7.7 μl, 81 μmol, 1 equiv) was mixed in dry DMF (200 μl) under nitrogen atmosphere and EtOH (300 μl) was added followed by $NaBH_4$ (2.5 mg, 66 μmol, 0.8 equiv). After stirring for 40 min at room temperature the solution was cooled to 0 °C and **2** (25 mg, 81 μmol) was added. Stirring was continued for 15 min at °0C and 25 min at room temperature. DCM (2 ml) was added and the solution was extracted with water (3 × 2 ml). The aqueous solution was evaporated to dryness and the residue was purified by a RP-silica column using water/acetonitrile (95:5, v/v) as an eluent. The product fractions were combined and evaporated to dryness to give **6** as a yellow crystalline solid (17 mg, 63%). ^{1}H NMR δ_H (500 MHz, D_2O): 4.78 (d, J = 6.9 Hz, 1H), 4.40 (dd, J = 5.5 and 6.9 Hz, 1H), 4.14 (dd, J = 4.5 and 5.5 Hz, 1H), 3.98 (m, 1H), 3.77 (dd, J = 3.8 and 12.3 Hz, 1H), 3.72 (dd, J = 5.6 and 12.3 Hz, 1H), 2.51 (s, 3H). ^{13}C NMR δ_C (125 MHz, D_2O): 170.7, 170.3, 142.0, 137.2, 85.0, 76.9, 73.5, 71.7, 61.9, 6.8. HRMS (ESI) *m/z*: [M − H]$^-$ calcd for $C_{10}H_{12}NO_6Se^-$ 321.9835; found 321.9834.

***Iso*-showdomycin-5′-triphosphate (7)/General procedure for triphosphorylation of nucleosides.** Freshly distilled phosphoryl chloride (18 μl, 0.20 mmol) and dry 2,4,6-trimethylpyridine (17 μl, 0.13 mmol) were added to a cooled (−10 °C) vigorously stirred solution of **1** (29.9 mg, 130 μmol) in dry triethyl phosphate (0.90 ml) under nitrogen atmosphere. The stirring was continued for 1.5 h at −10 °C (or 20 h at −10 °C − +4 °C in case of **2**−**7**). The reaction mixture was cooled to 0 °C and a dry solution of tris(tetrabutylammonium) hydrogen pyrophosphate (235 mg, 0.26 mmol) in MeCN (2 ml) and dry tributylamine (62 μl, 0.26 mmol) were added. The resulting solution was stirred for further 20 h at 0 °C − RT. 0.05 M solution of triethylammonium acetate (pH 7.0) (3.5 ml) and chloroform (3.5 ml) were added and stirring of the mixture was continued for 30 min. The aqueous phase of the heterogeneous mixture was separated and washed two times with chloroform (14 ml). NaI (80 mg) and acetone (22 ml) were added to the separated aqueous phase and the mixture was vortexed and cooled at 0 °C for 30 min. The precipitated phosphate products were collected by centrifugation. Final purification of the crude material was carried out by RP-HPLC (a Phenomemex Kinetex™ column, C18, 250 × 10 mm, 5 μm, flow rate 3 ml min- [1], eluted with a linear gradient from aqueous 0.025 M TEAA to 0.025 M TEAA in acetonitrile/H_2O, 70:30, *v/v*, over 20 min). The product fractions were lyophilized to yield a triethylammonium salt of **7** (5.6 μmol, 4.4%). ^{1}H NMR δ_H (500 MHz, D_2O): = 5.20 (d, 1H, J = 5.5 Hz), 4.52 (m, 1H), 4.39 (dd, J = 5.5 and 6.5 Hz, 1H), 4.27−4.22 (m, 1H), 4.16−4.11 (m, 1H), 3.39 (d, J = 21.7 Hz, 1H), 3.28 (d, J = 21.7 Hz, 1H). ^{13}C NMR δ_C (125 MHz, CD_3OD): 179.2, 173.4, 166.3, 100.1, 85.2 (d, J = 8.5 Hz), 69.7, 69.6, 64.2 (d, J = 5.4 Hz), 32.6.^{31}P NMR δ_P (202 MHz, D_2O): 10.94 (d, J = 20.0 Hz), − 11.54 (d, J = 20.0 Hz), − 23.35 (pseudo-t., J = 20.0 Hz). HRMS (ESI) *m/z*: [M − H]$^-$ calcd for $C_9H_{13}NO_{15}P_3^-$ 467.9504; found 467.9511.

Showdomycin-5′-phosphate (8). Freshly distilled phosphoryl chloride and dry 2,4,5-trimethylpyridine were added to a vigorously stirred solution of **1** (15 mg, 65 μmol) in dry triethylphosphate (0.4 ml) at −10 °C under nitrogen. The reaction was stirred for 1.5 h and then quenched by adding 0.05 M solution of triethylammonium acetate (pH 7.0) (1.5 ml) and chloroform (1.5 ml). The aqueous layer was separated and washed twice with chloroform (1.5 ml). NaI (40 mg) and acetone (10 ml) were added to the aqueous phase. The mixture was vortexed and cooled until the solid precipitate had formed. The precipitate was dissolved in water and purified by RP-HPLC (a Phenomemex Kinetex™ column, C18, 250 × 10 mm, 5 μm, flow rate 3 ml min- [1], eluted with a linear gradient from aqueous 0.025 M TEAA to 0.025 M TEAA in acetonitrile/H_2O, 70:30, *v/v*, over 17 min). The product fractions were lyophilized to obtain triethylammonium salt of **8** (27 μmol, 42%). ^{1}H NMR δ_H (500 MHz, D_2O): 6.70 (d, J = 1.5 Hz), 4.76 (dd, J = 1.5 Hz, 4.3 Hz, 1H), 4.24 (pseudo-t, J = 4.3 Hz, 1H), 4.15 (pseudo-t, J = 4.3 Hz, 1H) 4.10 (m, 1H), 4.09−4.04 (m, 1H), 3.97−3.92 (m, 1H). ^{13}C NMR δ_C (125 MHz, D_2O): 173.2, 172.5, 147.3, 129.1, 81.7 (d, J = 8.2 Hz), 77.6, 74.5, 70.6, 64.5 (d, J = 5.2 Hz). ^{31}P NMR δ_P (202 MHz, D_2O): 0.2 (s). HRMS (ESI) *m/z*: [M − H]$^-$ calcd for $C_9H_{11}NO_9P^-$ 308.0177; found 308.0174.

4-Bromoshowdomycin-5′-triphosphate (9). 2 (29 mg, 93 μmol) was phosphorylated according to the general procedure with the exception that the compound was not purified by HPLC. The product was not stable during lyophilisation of the TEAA buffered HPLC fractions. The pyrophosphate impurities were removed by treating the crude material with pyrophosphatase and the crude was precipitated from acetone by adding NaI, to obtain the sodium salt of **9** (8.5 μmol 9.2%). ^{1}H NMR δ_H (500 MHz, D_2O): = 4.82 (d, 1H, J = 6.75 Hz), 4.49 (dd, J = 5.50 and 6.75 Hz, 1H), 4.30 (dd, J = 4.41 and 5.50 Hz, 1H), 4.18 (m, 1H), 4.14−4.10 (m, 2H). ^{13}C NMR δ_C (125 MHz, CD_3OD): 170.1, 167.4, 139.6, 129.2, 83.5 (d, J = 9.2 Hz), 76.3, 73.5, 71.4, 65.7 (d, J = 5.9 Hz). ^{31}P NMR δ_P (202 MHz, D_2O): 10.63 (d, J = 19.2 Hz), − 11.15 (d, J = 19.2 Hz), − 22.76 (pseudo-t., J = 19.2 Hz). HRMS (ESI) *m/z*: [M − H]$^-$ calcd for $C_9H_{12}BrNO_{15}P_3^-$ 545.8609; found 545.8607.

4.1. 4-Methylthioshowdomycin-5′-triphosphate (10)

3 (30 mg, 109 μmol) was phosphorylated according to the general procedure to obtain the triethylammonium salt of methylthio-showdomycin-5′-triphosphate **10** (6.8 μmol, 6.2%). ^{1}H NMR δ_H (500 MHz, D_2O): = 4.80 (d, 1H, J = 7.12 Hz), 4.51 (dd, J = 5.68 and 7.08 Hz, 1H), 4.28 (dd, J = 3.86 and 5.68 Hz, 1H), 4.14−4.05 (overlapping, 2H), 4.11 (overlapping, 1H), 3.14 (TEA), 2.67 (s, 3H), 1.22 (TEA). ^{13}C NMR δ_C (125 MHz, D_2O): 170.7, 169.2, 146.2, 130.7, 83.5 (d, J = 9.2 Hz), 75.5, 72.6, 71.2, 65.6 (d, J = 6.0 Hz), 14.6.^{31}P NMR δ_P (202 MHz, D_2O): 10.28 (broad signal), − 11.33 (d, J = 19.9 Hz), − 23.36 (pseudo-t., J = 19.9 Hz). HRMS (ESI) *m/z*: [M − H]$^-$ calcd for $C_{10}H_{15}NO_{15}P_3S^-$ 513.9381; found 513.9356.

4-Ethylthioshowdomycin-5′-triphosphate (11). 4 (30 mg, 104 μmol) was phosphorylated according to the general procedure to obtain triethylammonium salt of **11** (4.6 μmol, 4.4%). ^{1}H NMR δ_H (500 MHz, D_2O): = 4.80 (d, 1H, J = 6.98 Hz), 4.52 (dd, J = 5.69 and 6.90 Hz, 1H), 4.28 (dd, J = 3.98 and 5.60 Hz, 1H), 4.15−4.05 (overlapping, 2H), 3.34−3.18 (m, 2H) 4.13 (overlapping, 1H), 3.14 (TEA), 1.26 (t, J = 7.40 Hz, 3H), 1.22 (TEA). ^{13}C NMR δ_C (125 MHz, CD_3OD): 170.5, 169.2, 145.2, 133.0, 83.5 (d, J = 8.9 Hz), 75.6, 72.7, 71.3, 65.7 (d, J = 5.8 Hz), 26.4, 15.0.^{31}P NMR δ_P (202 MHz, D_2O): 10.89 (d, J = 19.8 Hz), − 11.34 (d, J = 19.8 Hz), − 23.31 (pseudo-t., J = 19.8 Hz) HRMS (ESI) *m/z*: [M − H]$^-$ calcd for $C_{11}H_{17}NO_{15}P_3S^-$ 527.9537; found 527.9536.

4-Methylselenoshowdomycin-5′-triphosphate (12). 6 (17 mg, 53 μmol) was phosphorylated according to the general procedure.

RP-HPLC purified final product was precipitated in acetone by adding NaI to give sodium salt of **12** (8.0 μmol, 15%). ^{1}H NMR δ_H (500 MHz, D_2O): = 4.77 (d, 1H, J = 6.9 Hz), 4.46 (dd, J = 5.8 and 6.9 Hz, 1H), 4.26 (m, 1H), 4.15–4.10 (m, 3H). ^{13}C NMR δ_C (125 MHz, CD_3OD): 170.7, 170.5, 142.0, 136.6, 83.7 (d, J = 8.9 Hz), 76.6, 72.9, 71.1, 65.5 (d, J = 5.9 Hz), 6.7.^{31}P NMR δ_P (202 MHz, D_2O): −10.95 (d, J = 19.9 Hz), −11.40 (d, J = 19.9 Hz), − 23.36 (pseudo-t., J = 19.9 Hz). HRMS (ESI) *m/z*: [M − H]$^-$ calcd for $C_{10}H_{15}NO_{15}P_3Se^-$ 561.8825; found 561.8845.

4-(((1*R*)-1-carboxyethyl)thio)showdomycin-5′-triphosphate (13a). The crude material of triphosphate **9** (prepared from **2**, 21 mg, 68 μmol), was suspended in triethylphosphate/DMSO (1:1) (0.5 ml) and thiolactic acid (3 μl, 34 μmol) and DIEA (18 μl, 103 μmol) were added. The reaction was allowed to proceed for 4 h and 0.05 M solution of triethylammonium acetate (pH 7.0) (2 ml) and chloroform (2 ml) were added. The aqueous phase of the heterogeneous mixture was separated and washed with chloroform (2 × 2 ml). NaI (60 mg) and acetone (10 ml) were added to the separated aqueous phase. The mixture was vortexed and cooled down (to 0 °C) until the phosphate products were precipitated. Precipitated product mixture was collected by centrifugation and purified by RP-HPLC (a Phenomemex Kinetex™ column, C18, 250 × 10 mm, 5 μm, flow rate 3 ml min- [1], eluted with a linear gradient from aqueous 0.025 M TEAA to 0.025 M TEAA in acetonitrile/H_2O, 70:30, *v/v*, over 20 min). The product fractions were lyophilized to a small volume. Acetone and NaI were added to give precipitated sodium salt of the faster eluting isomer **13a** (2.0 μmol, 2.9% yield). ^{1}H NMR δ_H (500 MHz, D_2O): = 4.83 (d, J = 6.6 Hz, H1), 4.46–4.49 (m, 2H), 4.33 (dd, J = 4.5 and 5.7 Hz, 1H), 4.16–4.04 (m, 3H), 1.43 (d, J = 7.4 Hz, 3H). ^{13}C NMR δ_C (125 MHz, D_2O): 179.0, 170.2, 168.7, 145.0, 134.1, 83.4 (d, J = 8.8 Hz), 76.3, 72.9, 71.1, 65.5 (d, J = 5.5 Hz), 46.9, 19.0.^{31}P NMR δ_P (202 MHz, D_2O): −5.80 (d, J = 19.9 Hz), −10.75 (d, J = 19.9 Hz), − 21.63 (pseudo-t., J = 19.9 Hz). HRMS (ESI) *m/z*: [M − H]$^-$ calcd for $C_{12}H_{17}NO_{17}P_3S^-$ 571.9436; found 571.9432.

4-(((1*S*)-1-carboxyethyl)thio)showdomycin-5′-triphosphate (13b). Sodium salt of the slower eluting isomer **13b** (4.1 μmol, 6.0% yield) was obtained analogously as described for **13a**. ^{1}H NMR δ_H (500 MHz, D_2O): = 4.79 (d, J = 7.0 Hz, H1), 4.57–4.50 (m, 2H), 4.31 (dd, J = 4.2 and 5.7 Hz, 1H), 4.17–4.06 (m, 3H), 1.43 (d, J = 7.3 Hz, 3H). ^{13}C NMR δ_C (125 MHz, D_2O): 179.0, 170.5, 168.9, 144.7, 133.8, 83.6 (d, J = 8.0 Hz), 75.8, 72.7, 71.1, 65.6 (d, J = 5.6 Hz), 46.6, 18.4.^{31}P NMR δ_P (202 MHz, D_2O): −5.98 (d, J = 19.3 Hz), −10.77 (d, J = 19.3 Hz), − 21.68 (pseudo-t., J = 19.3 Hz). HRMS (ESI) *m/z*: [M − H]$^-$ calcd for $C_{12}H_{17}NO_{17}P_3S^-$ 571.9436; found 571.9421.

Nucleoside triphosphate concentration analysis. The molar amounts of the nucleoside triphosphates were assayed by titrating corresponding NMR-samples with a solution of acetonitrile (2%) in D_2O (3 × 10 μl) and acquiring ^{1}H NMR spectra with a relaxation delay (d1) of 30 s. The amounts of substances were calculated by comparing the nucleotide proton signal peak areas to that of the acetonitrile CH_3 singlet peak.

Antimicrobial activity measurements. Antimicrobial activity of the compounds was analysed by cultivating *E. coli* K-12 carrying plasmid p*EGFPluxABCDEamp* (*E. coli*/p*lux*) [25]. The plasmid expresses modified *luxABCDE* genes and the growth was followed by measuring bioluminescense (counts per second) and OD_{600} using Hidex Sense Plate Reader 425–301 (Hidex, Turku, Finland). Bacteria were first inoculated from glycerol stock (0.2% inocula) in LB containing 100 μg/ml ampicillin and mixed with the analysed compound to final concentration of 2.5–0.002 mM on 96 well plates (PerkinElmer 6005020) and incubated at 37 °C for 16 h in the luminometer used for measurements. The amount of uridine used in assays was 12.5–0.002 mM. Kanamycin and apramycin were purchased, pseudouridimycin was prepared in our laboratory [30].

Transcription elongation complex assembly. *Eco* and *Hsa* MT RNAP TECs (1 μM) were assembled by a procedure developed by Komissarova et al., 2003 [31]. An RNA primer was annealed to the template DNA, incubated with 1.5 μM RNAP for 10 min in TB buffer (40 mM HEPES-KOH pH 7.5, 80 mM KCl, 5% glycerol, 0.1 mM EDTA, and 0.1 mM DTT), and with 2 μM of the non-template DNA for 20 min at 25 °C. *Sce* RNAPII TECs were assembled as described above except that the incubation time after the addition of the non-template DNA was 10 min.

***In vitro* transcription reactions, single nucleotide addition assay.** Transcription reactions were initiated by the addition of 10 μl of NTPs and/or triphosphorylated showdomycin derivatives in TB10 buffer (TB buffer supplemented with 10 mM $MgCl_2$) to 10 μl of the assembled TEC in TB10 buffer. The final concentrations of the TEC, NTPs and triphosphorylated showdomycin derivatives were 0.1 μM, 20 μM and 100 μM, respectively. The reactions were incubated for 1 min at 25 °C and quenched with 30 μl of Gel Loading Buffer (94% formamide, 20 mM Li_4-EDTA and 0.2% Orange G). RNAs were separated on 16% denaturing polyacrylamide gels and visualized with an Odyssey Infrared Imager (Li-Cor Biosciences, Lincoln, NE); band intensities were quantified using the ImageJ software [32].

***In vitro* transcription reactions, processive transcript elongation.** Transcription reactions were initiated by the addition of 10 μl of ATP, CTP, GTP and UTP in TB10 buffer to 10 μl of the assembled TEC in TB10 buffer. The NTPs solution was supplemented with triphosphorylated showdomycin derivatives were indicated. The final concentrations of the TEC, NTPs and triphosphorylated showdomycin derivatives were 0.5 μM, 100 μM each, and 2 mM, respectively. The reactions were incubated for 5 min at 25 °C and quenched with 40 μl of Gel Loading Buffer. RNAs were separated on 16% denaturing polyacrylamide gels, visualized and quantified as described above.

Cytotoxicity and cell viability assays. Human embryonic kidney 293T (ACC 635) cells were obtained from Leibniz-Institut DSMZ GmbH. The cells were cultured in Dulbecco's modified eagle's medium (Lonza) supplemented with 10% fetal calf serum (Biowest), 2 mM L-glutamine (Lonza), 100 units/ml Pen-Strep (Lonza) and incubated at 37 °C in a humidified atmosphere of 5% CO^2. To analyze cytotoxicity and cell viability, CyQUANT™ LDH Cytotoxicity Assay Kit (Invitrogen) and Cell Counting Kit-8 (Dojindo) were used according to the manufacturer's instructions. Briefly, 7000 cells per well were added in a 96-well plate. Following 24 h incubation, increasing concentrations of SDM and EtSSDM (0–1000 μM) were added to the culture media in triplicates. After 24 h, absorbance at either 490 nm and 680 nm or 450 nm were detected using a microplate reader Multiscan GO (Thermo Scientific). The assays where repeated three times to collect the data presented in the results section. Samples were imaged by an EVOS M5000 Imaging System (Thermo Fisher Scientific) using a 20 x objective.

Author contributions

P.R. carried out production and chemical modification of compounds. J.J.M. conducted the *in vitro* transcription assays. K.P. carried out the *in vivo* antimicrobial assays. R.K.P. contributed to the development of transcription assays. K.P. and J.J. performed the cytotoxicity and cell proliferation assays. H.J.K., P.V., G.A.B. and M.M.-K. supervised the experiments. P.R., J.J.M. and K.P. wrote the manuscript, and all authors revised the manuscript.

Declaration of competing interest

The authors declare that they have no known competing financial interests or personal relationships that could have appeared to influence the work reported in this paper.

Acknowledgment

This work was supported by the Sigrid Jusélius Foundation (to M.M.-K. and G.A.B.), and Instrumentarium Science Foundation (to J.J.M). We wish to thank Janne Atosuo for his help in antimicrobial assays and providing the *E. coli*/p*lux* strain.

Appendix A. Supplementary data

Supplementary data to this article can be found online at https://doi.org/10.1016/j.ejmech.2022.114342.

Abbreviations

CPS	counts per second
DIEA	*N*,*N*-diisopropylethylamine;
DMF	*N*,*N*-dimethylformamide;
DMSO	dimethyl sulfoxide;
DTNB	5,5′-dithiobis(2-nitrobenzoic acid)
Eco	*Escherichia coli*
FMN	flavin mononucleotide;
GSH	glutathione
Hsa	*Homo sapiens*
LDH	lactate dehyrdorgenase
NTP	nucleoside triphosphate
RNA	ribonucleic acid
RNAP	RNA polymerase
RP-HPLC	reverse-phase high-performance liquid chromatography
RT	room temperature
Sce	*Saccharomyces cerevisiae*;
TEC	transcription elongation complex
THF	tetrahydrofuran

References

[1] C.M. Galmarini, J.R. Mackey, C. Dumontet, Nucleoside analogues: mechanisms of drug resistance and reversal strategies, Leukemia 15 (6) (2001) 875–890, https://doi.org/10.1038/sj.leu.2402114.
[2] E. De Clercq, C-nucleosides to Be revisited, J. Med. Chem. 59 (6) (2016) 2301–2311, https://doi.org/10.1021/acs.jmedchem.5b01157.
[3] K. Temburnikar, K.L. Seley-Radtke, Recent advances in synthetic approaches for medicinal chemistry of C-nucleosides, Beilstein J. Org. Chem. 14 (2018) 772–785, https://doi.org/10.3762/bjoc.14.65.
[4] S.I. Maffioli, Y. Zhang, D. Degen, T. Carzaniga, G. Del Gatto, S. Serina, P. Monciardini, C. Mazzetti, P. Guglierame, G. Candiani, A.I. Chiriac, G. Facchetti, P. Kaltofen, H.G. Sahl, G. Dehò, S. Donadio, R.H. Ebright, Antibacterial nucleoside-analog inhibitor of bacterial RNA polymerase, Cell 169 (7) (2017) 1240–1248, https://doi.org/10.1016/j.cell.2017.05.042, e23.
[5] D. Siegel, H.C. Hui, E. Doerffler, M.O. Clarke, K. Chun, L. Zhang, S. Neville, E. Carra, W. Lew, B. Ross, Q. Wang, L. Wolfe, R. Jordan, V. Soloveva, J. Knox, J. Perry, M. Perron, K.M. Stray, O. Barauskas, J.Y. Feng, Y. Xu, G. Lee, A.L. Rheingold, A.S. Ray, R. Bannister, R. Strickley, S. Swaminathan, W.A. Lee, S. Bavari, T. Cihlar, M.K. Lo, T.K. Warren, R.L. Mackman, Discovery and synthesis of a phosphoramidate prodrug of a pyrrolo[2,1-f][triazin-4-amino] adenine C-nucleoside (GS-5734) for the treatment of ebola and emerging viruses, J. Med. Chem. 60 (5) (2017) 1648–1661, https://doi.org/10.1021/acs.jmedchem.6b01594.
[6] T.K. Warren, J. Wells, R.G. Panchal, K.S. Stuthman, N.L. Garza, S.A. Van Tongeren, L. Dong, C.J. Retterer, B.P. Eaton, G. Pegoraro, S. Honnold, S. Bantia, P. Kotian, X. Chen, B.R. Taubenheim, L.S. Welch, D.M. Minning, Y.S. Babu, W.P. Sheridan, S. Bavari, Protection against filovirus diseases by a novel broad-spectrum nucleoside analogue BCX4430, Nature 508 (7496) (2014) 402–405, https://doi.org/10.1038/nature13027.
[7] S. Roy-Burman, P. Roy-Burman, D.W. Visser, Showdomycin, A new nucleoside antibiotic, Cancer Res. 28 (8) (1968) 1605–1610.
[8] T. Müller, E. Bause, L. Jaenicke, Glycolipid formation in volvox carteri f. Nagariensis. Effects of tunicamycin and showdomycin, FEBS Lett. 128 (2) (1981) 208–212, https://doi.org/10.1016/0014-5793(81)80082-8.
[9] H. Nishimura, M. Mayama, Y. Komatsu, H. Kato, N. Shimaoka, Y. Tanaka, Showdomycin, a New Antibiotic from a Streptomyces SP, J. Antibiot., Tokyo), 1964.
[10] S. Matsuura, O. Shiratori, K. Katagiri, Antitumor activity of showdomycin, J. Antibiot. 17 (1964) 234–237.
[11] C.E. Cass, N. Kolassa, Y. Uehara, E. Dahlig-Harley, E.R. Harley, A.R.P. Paterson, Absence of binding sites for the transport inhibitor nitrobenzylthioinosine on nucleoside transport-deficient mouse lymphoma cells, BBA - Biomembr 649 (3) (1981) 769–777, https://doi.org/10.1016/0005-2736(81)90182-6.
[12] Y. Uehara, J.M. Fisher, M. Rabinovitz, Showdomycin and its reactive moiety, maleimide: a comparison in selective toxicity and mechanism of action in vitro, Biochem. Pharmacol. 29 (16) (1980) 2199–2204, https://doi.org/10.1016/0006-2952(80)90198-7.
[13] T. Tobin, T. Showdomycin Akera, A nucleotide-site-directed inhibitor of (Na++ K+)-ATPases, Biochim. Biophys. Acta 389 (1975) 126–136.
[14] T.I. Kalman, Inhibition of thymidylate synthetase by showdomycin and its 5'-phosphate, Biochem. Biophys. Res. Commun. 49 (4) (1972) 1007–1013.
[15] T. Böttcher, S.A. Sieber, Showdomycin as a versatile chemical tool for the detection of pathogenesis-associated enzymes in bacteria, J. Am. Chem. Soc. 132 (20) (2010) 6964–6972, https://doi.org/10.1021/ja909150y.
[16] J. Arendes, R.K. Zahn, E. Hantke, W.E.G. Müller, Degradation and intracellular phosphorylation of showdomycin, Cancer Lett. 4 (1978) 259–264.
[17] H. Mosaei, J. Harbottle, Mechanisms of antibiotics inhibiting bacterial RNA polymerase, Biochem. Soc. Trans. 47 (1) (2019) 339–350, https://doi.org/10.1042/BST20180499.
[18] C. Ma, X. Yang, P.J. Lewis, Bacterial transcription as a target for antibacterial drug development, Microbiol. Mol. Biol. Rev. 80 (1) (2016) 139–160, https://doi.org/10.1128/mmbr.00055-15.
[19] R.K. Prajapati, P. Rosenqvist, K. Palmu, J.J. Mäkinen, A.M. Malinen, P. Virta, M. Metsä-Ketelä, G.A. Belogurov, Oxazinomycin arrests RNA polymerase at the polythymidine sequences, Nucleic Acids Res. 47 (19) (2019) 10296–10312, https://doi.org/10.1093/nar/gkz782.
[20] D. Maryanka, I.R. Johnston, The inhibition of DNA-dependent RNA polymerase of E. Coli by showdomycin, FEBS Lett. 7 (2) (1970) 125–128.
[21] K. Palmu, P. Rosenqvist, K. Thapa, Y. Ilina, V. Siitonen, B. Baral, J. Mäkinen, G. Belogurov, P. Virta, J. Niemi, M. Metsä-Ketelä, Discovery of the showdomycin gene cluster from Streptomyces showdoensis ATCC 15227 yields insight into the biosynthetic logic of C-nucleoside antibiotics, ACS Chem. Biol. 12 (6) (2017) 1472–1477, https://doi.org/10.1021/acschembio.7b00078.
[22] H. Nishimura, Antibiotic Showdomycin and a Method of Producing Same, 1967. Patent US3316149.
[23] M. Yoshikawa, T. Kato, T. Takenishi, Studies of phosphorylation. III. Selective phosphorylation of unprotected nucleosides, Bull. Chem. Soc. Jpn. 42 (12) (1969) 3505–3508, https://doi.org/10.1246/bcsj.42.3505.
[24] M. Ozaki, Partial purification and properties of enzyme inactivating showdomycin from Streptomyces sp. No. 383, Agric. Biol. Chem. 44 (5) (1980) 997–1001, https://doi.org/10.1080/00021369.1980.10864087.
[25] J. Atosuo, J. Lehtinen, L. Vojtek, E.M. Lilius, Escherichia coli K-12 (PEGFPlux-ABCDEamp): a tool for analysis of bacterial killing by antibacterial agents and human complement activities on a real-time basis, Luminescence 28 (5) (2013) 771–779, https://doi.org/10.1002/bio.2435.
[26] H. Nishimura, Y. Komatsu, Reversal of inhibiting action of showdomycin on the proliferation of Escherichia coli by nucleosides and thiol compounds, J. Antibiot. 21 (4) (1968) 250–254, https://doi.org/10.7164/antibiotics.21.250.
[27] Y. Komatsu, Mechanism of action of showclomycin Part Iv interactions between the mechanisms for transport of showdomycin and of various nucleosides in Escherichia coli, Agric. Biol. Chem. 35 (9) (1971) 1328–1339, https://doi.org/10.1080/00021369.1971.10860080.
[28] T. Shiraishi, T. Kuzuyama, Recent advances in the biosynthesis of nucleoside antibiotics, J. Antibiot. (Tokyo) 72 (12) (2019) 913–923, https://doi.org/10.1038/s41429-019-0236-2.
[29] P.W. Riddles, R.L. Blakeley, B. Zerner, Reassessment of Ellman's reagent, Methods Enzymol. 91 (C) (1983) 49–60, https://doi.org/10.1016/S0076-6879(83)91010-8.
[30] P. Rosenqvist, K. Palmu, R.K. Prajapati, K. Yamada, J. Niemi, G.A. Belogurov, M. Metsä-Ketelä, P. Virta, Characterization of C-nucleoside antimicrobials from Streptomyces albus DSM 40763: strepturidin is pseudouridimycin, Sci. Rep. 9 (1) (2019) 1–9, https://doi.org/10.1038/s41598-019-45375-w.
[31] N. Komissarova, M.L. Kireeva, J. Becker, I. Sidorenkov, M. Kashlev, Engineering of elongation complexes of bacterial and yeast RNA polymerases, Methods Enzymol. 371 (2003) 233–251, https://doi.org/10.1016/S0076-6879(03)71017-9, 1997.
[32] M.D. Abràmoff, P.J. Magalhães, S.J. Ram, Image processing with ImageJ Part II, Biophot. Int. 11 (7) (2005) 36–43.